Mechanism of the Hydrogen Transfer from the OH Group to Oxygen-Centered Radicals: Proton-Coupled Electron-Transfer versus Radical Hydrogen Abstraction

Santiago Olivella,*[a] Josep M. Anglada,*[a] Albert Solé,[b] and Josep M. Bofill[c]

Abstract: High-level ab initio electronic structure calculations have been carried out with respect to the intermolecular hydrogen-transfer reaction $HCOOH + {}^{\bullet}OH \rightarrow HCOO^{\bullet} + H_2O$ and the intramolecular hydrogen-transfer reaction ${}^{\bullet}OOCH_2OH \rightarrow HOOCH_2O^{\bullet}$. In both cases we found that the hydrogen atom transfer can take place via two different transition structures. The lowest energy transition structure involves a proton transfer coupled to an electron transfer from the ROH species to the radical, whereas the higher energy transition structure corresponds to the conventional radical hydrogen atom abstraction. An analysis of the atomic spin population, computed within the framework of the topological theory of atoms in molecules, suggests that the triplet repulsion between the unpaired electrons located on the oxygen atoms that undergo hydrogen exchange must be much higher in the transition structure for the radical hydrogen abstraction than that for the proton-coupled electron-transfer mechanism. It is suggested that, in the gas phase, hydrogen atom transfer from the OH group to oxygen-centered radicals occurs by the proton-coupled electron-transfer mechanism when this pathway is accessible.

Keywords: ab initio calculations · atmospheric chemistry · hydrogen transfer · radical reactions · reaction mechanisms

Introduction

Hydrogen-transfer reactions from the OH group to oxygen-centered radicals [Eq. (1)] play an important role in various complex systems, especially in the chemical degradation of many organic molecules in the troposphere[1] and also in combustion chemistry.[2]

$$RO{-}H + {}^{\bullet}OR' \rightarrow RO^{\bullet} + H{-}OR' \quad (1)$$

From a general point of view, the reactions depicted in Equation (1) are a subclass of more general hydrogen atom abstraction reactions by free radicals [Eq. (2)].

$$X{-}H + {}^{\bullet}Y \rightarrow X^{\bullet} + H{-}Y \quad (2)$$

It is generally accepted that such reactions proceed by the concerted breaking and making of strong covalent chemical bonds to the transferring atom (i.e., X–H and Y–H); as the radical ${}^{\bullet}Y$ approaches the X–H bond with its unpaired electron, the Y–H bond is formed, while the X–H bond is homolytically broken. This implies the formation of a three-center three-electron bond in the transition structure, in which the unpaired electron of the radical is delocalized over X, H, and Y. Another common belief is that the energy barrier for the transfer of a hydrogen atom between X and Y depends on the triplet repulsion energy for the $X^{\bullet}/Y^{\bullet}$ pair at the transition structure.[3–5] This is caused by the necessary occurrence of parallel electron spins on X and Y during the course of the hydrogen-transfer reaction, namely, $[X\uparrow\cdots H\downarrow\cdots Y\uparrow]^{\ddagger}$.

[a] Prof. S. Olivella, Dr. J. M. Anglada
Institut d'Investigacions Químiques i Ambientals de Barcelona
CSIC, Jordi Girona 18, 08028-Barcelona, Catalonia (Spain)
Fax: (+34) 932-045-904
E-mail: sonqtc@iiqab.csic.es
jarqtc@iiqab.csic.es

[b] Dr. A. Solé
Centre Especial de Recerca en Química Teòrica
Departament de Química Física
Universitat de Barcelona, Martí i Franquès 1
08028-Barcelona, Catalonia (Spain)

[c] Dr. J. M. Bofill
Centre Especial de Recerca en Química Teòrica
Departament de Química Orgànica
Universitat de Barcelona, Martí i Franquès 1
08028-Barcelona, Catalonia (Spain)

Supporting information for this article is available on the WWW under http://www.chemeurj.org/ or from the author. (Cartesian coordinates of all structures reported in this paper, Tables S1–S6 summarize total energies, zero-point vibrational energies, and topological properties of bond critical points)

DOI: 10.1002/chem.200305714

For X=Y=O [i.e., Eq. (1)], the presence of lone pairs of electrons on the oxygen atoms may lead to a different approach of the reactants intending to avoid the triplet repulsion between the unpaired electrons centered at these atoms. This requires RO–H species with R carrying a terminal atom, Z, with a lone pair of electrons. In this case, in addition to the simple hydrogen atom transfer mechanism depicted in Scheme 1, one may envisage a situation involving a R–OH···OR′ hydrogen bond and a Z:···•OR′ two-center three-electron bond, as depicted in Scheme 2. Such an entity may react by undergoing a proton transfer coupled to the transfer of an electron from Z: to •OR′ (or the incipient $[HOR']^{\bullet+}$ species). The net result of this process is identical to that of a simple hydrogen atom transfer, except that the Z–R–O• species is left in a different electron configuration, with Z instead of O carrying the unpaired electron. Intramolecular electron transfer from O to Z• restores the :Z–R–O• entity.

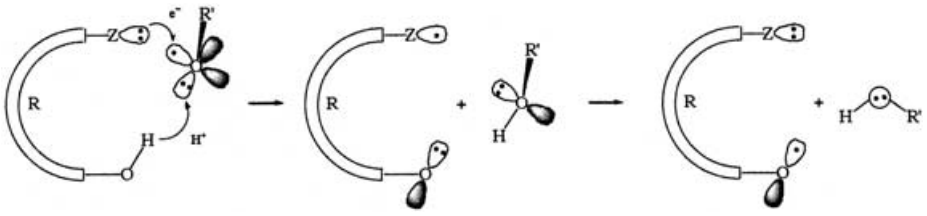

Scheme 2. Proton transfer from a R–OH species to an oxygen-centered radical •OR′ coupled to an electron transfer from R to •OR′. The oxygen 2p-type orbitals are represented by ∞ if in the plane of the paper and by ○ if perpendicular to this plane.

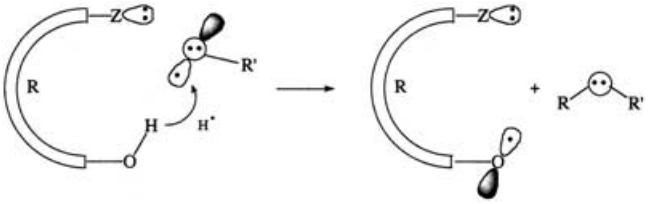

Scheme 1. Conventional hydrogen atom transfer from a R–OH species to an oxygen-centered radical •OR′. The oxygen 2p-type orbitals are represented by ∞ if in the plane of the paper and by ○ if perpendicular to this plane.

In this article, we wish to report the results of ab initio electronic structure calculations on two examples, one intermolecular and the other intramolecular, of hydrogen atom transfer from hydroxylic oxygen to oxygen-centered radicals, which is predicted to occur through a proton-coupled electron-transfer mechanism.[6] The first example is the abstraction of the acidic hydrogen atom of formic acid (HCOOH) by a hydroxyl radical (•OH) [Eq. (3)].

$$HCOOH + {}^{\bullet}OH \rightarrow HCOO^{\bullet} + H_2O \quad (3)$$

The second example is the intramolecular 1,4-hydrogen transfer in the peroxy radical •$OOCH_2OH$ [Eq. (4)].

$${}^{\bullet}OOCH_2OH \rightarrow HOOCH_2O^{\bullet} \quad (4)$$

Both reactions play a key role in environmental science. For the sake of comparison, the simplest bimolecular hydrogen atom transfer from hydroxylic oxygen to oxygen-centered radicals, namely the identity exchange reaction [Eq. (5)], has also been considered in this theoretical study.

$$H_2O + {}^{\bullet}OH \rightarrow HO^{\bullet} + H_2O \quad (5)$$

Abstract in Catalan: *S'han realitzat càlculs d'estructura electrònica ab initio d'alt nivell per la reacció de transferència d'hidrogen intermolecular $HCOOH + {}^{\bullet}OH \rightarrow HCOO^{\bullet} + H_2O$ i per la reacció de transferència d'hidrogen intramolecular ${}^{\bullet}OOCH_2OH \rightarrow HOOCH_2O^{\bullet}$. En abmdós casos trobem que la transferència de l'àtom d'hidrogen té lloc via dues estructures de transició diferents. L'estructura de transició d'energia més bixa implica una transferència de protó acoblada a la transferència d'un electró des de l'espècie ROH al radical, mentre que l'estructura de transició d'energia més alta correspon a una abstracció d'hidrogen radicalària convencional. Una anàlisi de les poblacions àtomiques d'spín electrònic, calculades en el marc de la teoria topològica d'àtoms en molècules, suggereix que la repulsió dels electrons no aparellats localitzats sobre els àtoms d'oxigen que experimenten el bescanvi d'hidrogen ha de ser molt més alta en l'estructura de transició per l'abstracció d'hidrogen radicalària que en l'estructura de transició del mecanisme de transferència de protó acoblada a la transferència d'un electró. Es suggereix que, en fase gas, les transferències de l'àtom d'hidrogen de l'OH a radicals d'oxigen tenen lloc per un mecanisme de transferència de protó acoblada a la transferència d'un electró quan aquest cami de reacció és accessible.*

Computational Methods

We optimized the geometries of the reactants and transition structures[7] for Equations (3)–(5) by means of analytical gradient procedures,[8] employing the (frozen core) quadratic configuration interaction with the singles and doubles method, based on a unrestricted Hartree–Fock (UHF) reference determinant,[9] designated UQCISD, in conjunction with the split-valence 6—311+G(2df,2p) basis set.[10] This basis set includes a single diffuse sp shell on carbon and oxygen atoms,[11] double d-polarization, as well as a single additional f-polarization on carbon and oxygen atoms, and double p-polarization on hydrogen atoms. To characterize the nature (minimum or saddle point) of the calculated stationary points and evaluate the zero-point vibrational energies (ZPVEs), the harmonic vibrational frequencies were computed. For Equation (5), the frequencies were calculated at the UQCISD/6-311+G(2df,2p) level. To lower the enormous computational cost involved in the calculation of the frequencies of the stationary points found for Equations (3) and (4) at this level of theory, the geometries and harmonic vibrational frequencies of these points were calculated with the (frozen core) second-order Møller–Plesset perturbation theory, based on a UHF reference determinant,[12] designated UMP2, with the 6-311+G(2df,2p) basis set. Moreover, we performed intrinsic reaction coordinate (IRC) calculations[13] on the transition structures to check their connection with the designated reactants

and products. All of these calculations were carried out with the GAUSSIAN 98 program package.[14]

Total energies were obtained from single-point (frozen core) coupled-cluster[15] calculations including all single and double excitations, based on a reference UHF single determinant, together with a perturbative treatment of all connected triple excitations,[16] designated UCCSD(T). In addition, total energies were also evaluated from partially spin-adapted CCSD(T) calculations based on a restricted open-shell Hartree–Fock (ROHF) reference determinant,[17] designated RCCSD(T), to accomplish the spin contamination problem in UCCSD(T) wave functions.[18] Both the UCCSD(T) and RCCSD(T) calculations were performed with the 6-311+G(2df,dp) basis set. Relative energies discussed in the text refer to energies computed at the RCCSD(T) theory level, unless stated otherwise. The UCCSD(T) calculations were carried out with GAUSSIAN 98, whereas MOLPRO 98[19] program package was employed for the RCCSD(T) calculations.

To examine the characteristics of the bonding and interactions in the most relevant structures, we also performed an analysis of the electron charge and electron spin density within the framework of the topological theory of atom in molecules (AIM)[20] making use of a locally modified version[21] of the PROAIM and EXTREME programs of Bader et al.[22] The Z density matrix obtained from UQCISD gradient calculations with the 6-311+G(2df,2p) basis set, an effective correlated density matrix,[23] was used in this analysis. The coefficients of selected natural orbitals generated from that density matrix were used to elucidate the topological nature of the molecular orbitals (MOs) describing the unpaired electron and the more relevant electron pairs.

Results and Discussion

Hydrogen atom transfer between two hydroxyl radicals: In good agreement with previous high-level ab initio calculations,[24–29] we found a transition structure with C_2 symmetry for Equation (5).[30] Selected geometrical parameters of this transition structure and atomic spin populations are shown in Figure 1.

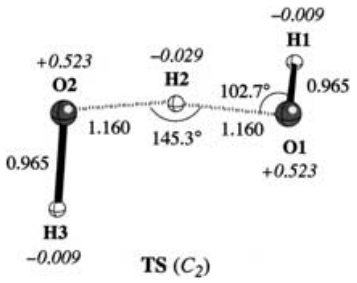

Figure 1. Selected parameters (bond lengths [Å] and angles [°]) of the UQCISD/6-311+G(2df,2p) optimized geometry of the transition structure for the hydrogen atom transfer between two hydroxyl radicals. Atomic spin populations from an AIM analysis, calculated by the same method, are given in italics.

The electronic state symmetry of the transition structure is ^{2}B. The coefficients of the natural orbital carrying the unpaired electron indicate that the spin population in the transition structure is concentrated on the two oxygen atoms which undergo hydrogen exchange, but shows a small negative value on the hydrogen atom being transferred. This result is consistent with a three-center three-electron bond and indicates that the transition structure of Equation (5) is of the hydrogen atom abstraction by radicals type.

On the basis of the large value of the spin population on the oxygen atoms that undergo hydrogen exchange, one would expect triplet repulsion between these atoms to be important in the transition structure, leading to a sizeable potential energy barrier for Equation (5). In fact, our calculations predict a barrier of 10.3 (UCCSD(T)) or 10.6 kcal mol^{-1} (RCCSD(T)) for this reaction, which is in reasonable agreement with the prediction of 9.6 kcal mol^{-1} obtained by Uchimaru et al.[29] from UCCSD(T) calculations with the aug-cc-pVQZ basis set. Inclusion of a thermal correction of the enthalpy of 2.2 kcal mol^{-1} (Table S1, Supporting Information), evaluated from the UQCISD/6-311+G(2df,2p) calculations, leads to a predicted activation enthalpy of $\Delta H^{\neq} = 8.4$ kcal mol^{-1} at 298 K. Furthermore, an Arrhenius activation energy of $E_a = 9.6$ kcal mol^{-1} at room temperature is obtained from $E_a = \Delta H^{\neq} + 2RT$. However, this is still much higher than the experimental $E_a = 4.2 \pm 0.5$ kcal mol^{-1}, determined over the temperature range 300–420 K.[31] For Equation (5), Uchimaru et al. have calculated a contribution to the Arrhenius activation energy of -4.6 kcal mol^{-1} arising from quantum-mechanical tunneling.[29] Therefore, the predicted Arrhenius activation energy would be further reduced to the value of 5.0 kcal mol^{-1}, which is in reasonable agreement with the experimental value given above.

Acidic hydrogen atom abstraction from formic acid by a hydroxyl radical: For Equation (3), we found two transition structures, designated **TS1** and **TS2**. Selected geometrical parameters and atomic spin populations of **TS1** and **TS2** are shown in Figure 2. Relative energies calculated at different levels of theory with the 6-311+G(2df,dp) basis set are summarized in Table 1, while the total energies and ZPVEs are collected in Table S3 in the Supporting Information. Calculated topological properties of the bond critical points for these transition structures are given in Table S4 in the Supporting Information. Structures **TS1** and **TS2** differ essentially in the orientation of the ·OH radical with respect to the molecular plane of the formic acid. While the O1−H1 bond is nearly orthogonal to that plane in **TS1**, it lies within that plane in **TS2**. The geometry of **TS2** is close to that of the planar transition structure reported by Galano et al.,[32] which was computed at the MP2, MP4, and QCISD theory levels with the 6-311++G(d,p) basis set. Moreover, the geometry of **TS1** is comparable to that of the nonplanar transition structure with a dihedral angle H1-O1-H2-O2 of $\approx 90°$ reported in the same study, which was obtained from

Table 1. Relative energies [kcal mol^{-1}] calculated at different levels of theory with the 6-311+G(2df,2p) basis set[a] of the reactants and the transition structures[b] for the acidic hydrogen atom abstraction from formic acid by a hydroxyl radical.

Species	UQCISD	UCCSD(T)	RCCSD(T)
HCOOH + ·OH	0.0	0.0	0.0
TS1	7.0	3.3	3.1
TS2	10.5	7.2	8.7

[a] With UQCISD/6-311+G(2df,2p) optimized geometries. [b] See Figure 2.

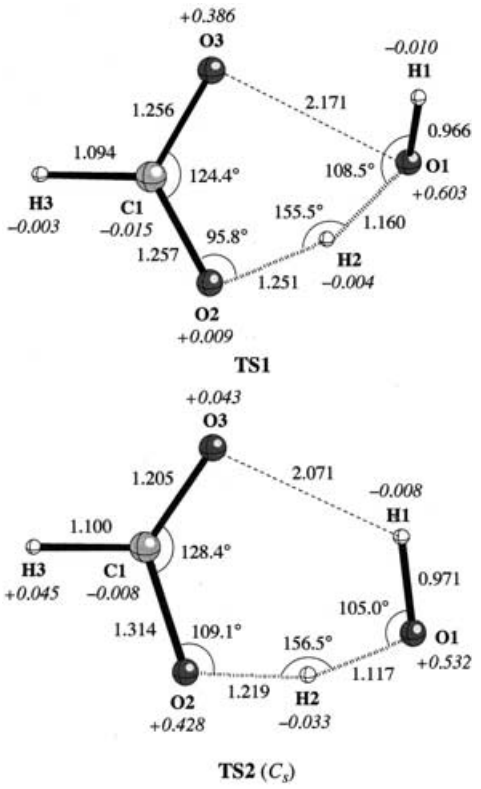

Figure 2. Selected parameters (bond lengths [Å] and angles [°]) of the UQCISD/6-311+G(2df,2p) optimized geometry of the two transition structures found for the acidic hydrogen atom abstraction from formic acid by hydroxyl radical. Atomic spin populations from an AIM analysis, calculated by the same method, are given in italics.

B3LYP and BH&HLP density functional theory (DFT) calculations with the 6-311++G(d,p) basis set. However, Galano et al. concluded that this nonplanar transition structure is an artifact of the DFT calculations, because they found that it has two imaginary frequencies both at the UMP2 and the UMP4 levels of theory. In contrast, we found **TS1** to be a true transition structure (i.e., only one imaginary frequency) at the UMP2 level of theory with the 6-311+G(2df,2p) basis set.

Table 1 shows that, at all levels of theory, the relative energy of **TS1** with respect to the reactants HCOOH + ·OH is lower than that of **TS2**. At first sight, this result is surprising, because, as noted by Galano et al.,[32] the short distance between H1 and O3 in **TS2** suggests a hydrogen-bond-like interaction that should lower the energy of this transition structure with respect to that of **TS1**. Actually, our AIM analysis of the electron charge density in **TS2** revealed the presence of a bond critical point located between the atoms H1 and O3, indicating that there is a bonding interaction between this atom pair. The low value of the electron charge density ($\rho(r_b) = 0.0226\ e\,bohr^{-3}$) and the positive value of the its Laplacian ($\nabla^2\rho(r_b) = 0.0808\ e\,bohr^{-5}$) and local electronic energy density ($E_e(r_b) = 0.0013$ hartree $bohr^{-3}$) calculated for this bond critical point (see Table S4, Supporting Information) is typically associated with interactions between closed-shell systems (e.g., hydrogen bonds). If Equation (3) were to take place via **TS2**, the hydrogen-bond-like interaction would explain the lower potential energy barrier calculated for this reaction (8.7 kcal mol^{-1}) compared to that calculated for Equation (5) (10.6 kcal mol^{-1}).

Now we address the question of why the energy of **TS1** is lower than that of **TS2**. As in the case of the transition structure found for Equation (5), Figure 2 shows that the spin population in **TS2** is concentrated on the oxygen atoms between which the hydrogen atom is being transferred with a small negative value (−0.033) on the hydrogen atom. In contrast, the spin population in **TS1** is concentrated on the oxygen atoms O1 and O3, whereas the spin population on atom O2 is negligible. From these results, it follows that the triplet repulsion between the unpaired electrons centered at the two oxygen atoms involved in the hydrogen atom transfer in **TS2** should be comparable to that of the transition structure of Equation (5), while this repulsion is expected to be negligible in **TS1**. Therefore, the lower energy of **TS1** compared to **TS2** can be mainly attributed to the lack of triplet repulsion between the two oxygen atoms involved in the hydrogen atom transfer in the former transition structure.

At this point one may wonder whether the high spin population on O1 and O3 in **TS1** might cause a triplet repulsion between these atoms. In this respect, it is worth noting that the AIM analysis of the electron charge density in **TS1** revealed the presence of a bond critical point located between the atoms O1 and O3, indicating that there is a bonding interaction between this atom pair. The small electron charge density ($\rho(r_b) = 0.0482\ e\,bohr^{-3}$) and the positive value of the its Laplacian ($\nabla^2\rho(r_b) = 0.1970\ e\,bohr^{-5}$) and local electronic energy density ($E_e(r_b) = 0.0036$ hartree $bohr^{-3}$) calculated for this bond critical point (see Table S4, Supporting Information) suggest that O1 and O3 are weakly bonded by a noncovalent interaction. What is the origin of this interaction? To answer this question we inspected the natural orbitals shown in Figure 3, which have electron occupancies of 1.9110 (bottom) and 1.0424 (top). Basically, these orbitals are two-center O3–O1 bonding and antibonding MOs, re-

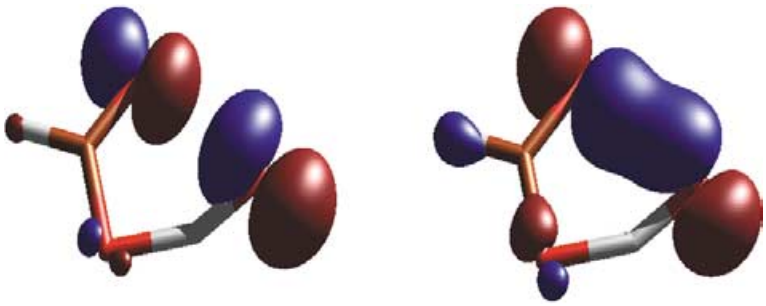

Figure 3. Representations of the natural orbitals having electron occupancies of 1.9110 (right) and 1.0424 (left) in the transition structure **TS1** for the acidic hydrogen atom abstraction from formic acid by hydroxyl radical.

spectively, arising from the interaction between a lone pair of electrons on O3 and the unpaired electron on O1. The result of such a two-center three-electron interaction is a weak bonding interaction between the reactants HCOOH and ·OH in the transition structure **TS1**. Most importantly, this interaction allows the transfer of a single electron from O3 to O1, which leads to double occupation of the initially singly occupied 2p-type orbital of the ·OH radical.

The remarkable feature of **TS1** is that it is not a transition structure of the conventional radical hydrogen abstraction type. From a qualitative point of view, the primary changes in bonding that occur in **TS1** can be described as those illustrated at the top of Scheme 3, in which we have ignored the 2s-type lone pair of electrons on the oxygen atoms, which are tightly bound; the curved arrows and semiarrows represent actual movement of electron pairs and single electrons, respectively. According to Scheme 3, during the course of the reaction, a proton and a single electron are transferred simultaneously from the formic acid to the hydroxyl radical. These electronic features indicate that the hydrogen atom transfer through **TS1** takes place by a proton-coupled electron-transfer mechanism. In contrast, the primary changes in bonding occurring in **TS2** can be described as the concerted breaking and making of the O2–H2 and O1–H2 bonds, respectively. These changes, depicted at the bottom of Scheme 3, indicate that the hydrogen atom transfer through **TS2** takes place by the conventional radical hydrogen abstraction mechanism.

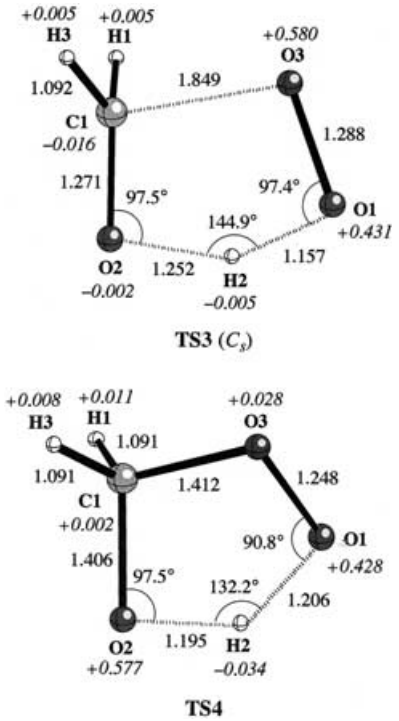

Figure 4. Selected parameters (bond lengths [Å] and angles [°]) of the UQCISD/6-311+G(2df,2p) optimized geometries of the two transition structures found for the intramolecular 1,4-hydrogen transfer in the peroxy radical ·$OOCH_2OH$. Atomic spin populations from an AIM analysis, calculated by the same method, are indicated in italics.

Intramolecular 1,4-hydrogen transfer in the peroxy radical ·$OOCH_2OH$: We found two transition structures, designated **TS3** and **TS4**, for the intramolecular 1,4-hydrogen transfer in the peroxy radical ·$OOCH_2OH$ [Eq. (4)]. Selected geometrical parameters and atomic spin populations of **TS3** and **TS4** are shown in Figure 4. Relative energies calculated at different levels of theory with the 6-311+G(2df,dp) basis set are summarized in Table 2, whereas the total energies and ZPVEs are collected in Table S5 in the Supporting Information. Calculated topological properties of the bond critical points for these transition structures are given in

Proton-coupled electron-transfer mechanism:

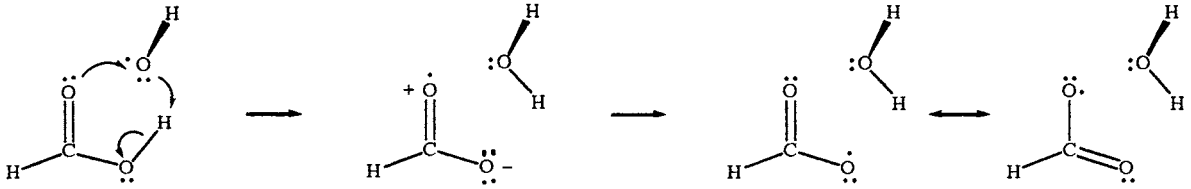

Hydrogen atom transfer mechanism:

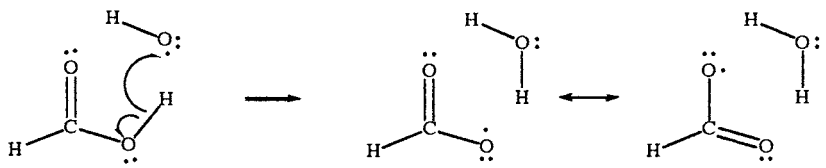

Scheme 3.

Table 2. Relative energies [kcal mol^{-1}] calculated at different levels of theory with the 6-311+G(2df,2p) basis set[a] of the reactants and the transition structures[b] for the intramolecular 1,4-hydrogen transfer in the peroxy radical $^{\bullet}OOCH_2OH$.

Species	UQCISD	UCCSD(T)	RCCSD(T)
$^{\bullet}OOCH_2OH$	0.0	0.0	0.0
TS3	22.0	18.2	18.1
TS4	54.0	45.7	48.7

[a] With UQCISD/6-311+G(2df,2p) optimized geometries. [b] See Figure 4.

Table S6 in the Supporting Information. Structure **TS3** shows a planar cyclic structure with an electronic symmetry state of $^2A''$. This transition structure involves the simultaneous transfer of the hydrogen atom of the OH group to the terminal oxygen atom of the peroxy radical $^{\bullet}OOCH_2OH$ and the breaking of the C1–O3 bond. Thus **TS3** leads to the concerted $HO_2^{\bullet}$ elimination from this peroxy radical, rather than to the alkoxy radical $HOOCH_2O^{\bullet}$. In contrast, **TS4** shows a puckered cyclic structure and involves only the transfer of the hydrogen atom of the OH group to the terminal oxygen atom of the peroxy radical $^{\bullet}OOCH_2OH$ to give the alkoxy radical $HOOCH_2O^{\bullet}$. As expected, the geometries of **TS3** and **TS4** are close to those found at the CASSCF(7,6) level of theory with the 6-311G(d,p) basis set, which we have reported previously.[33]

As shown in Table 2, at all levels of theory, the relative energy of **TS3** with respect to the reactant $^{\bullet}OOCH_2OH$ is lower than that of **TS4**. Evidently, the much higher energy of **TS4** relative to **TS3** arises mainly from the larger strain energy of the five-membered ring of the former transition structure.[33] However, there is an additional electronic feature that increases the energy of **TS4**, with respect to that of **TS3**, that can be traced to the atomic spin populations calculated for the two structures (see Figure 4). As in the case of the transition structure found for Equation (5), the spin population in **TS4** is concentrated on O1 and O2 with a small negative value on the hydrogen atom being transferred (H2). In clear contrast, the spin population in **TS3** is concentrated on O1 and O3, while the spin population on O2 and H2 is negligible. As a result, the triplet repulsion between the unpaired electrons centered at the two oxygen atoms involved in the hydrogen atom transfer in **TS4** and in the transition structure of Equation (5) should be comparable, while this repulsion is negligible in **TS3**. Therefore, the lower energy of **TS3** relative to **TS4** can be attributed, in part, to the lack of triplet repulsion between the two oxygen atoms involved in the hydrogen atom transfer in **TS3**.

From a qualitative point of view, the primary changes in bonding that occur in **TS3** are depicted at the top of Scheme 4. During the course of the reaction, a proton and a single electron are transferred simultaneously from the OCH_2OH moiety to the terminal oxygen of the peroxy group, O1. These electronic features indicate that the mechanism of the 1,4-hydrogen transfer in $^{\bullet}OOCH_2OH$ leading to the concerted $HO_2^{\bullet}$ elimination through **TS3** is of a proton-coupled electron-transfer type. In contrast, the primary changes in bonding occurring in **TS4** can be described as the concerted breaking and making of the O2–H2 and O1–H2 bonds, respectively. These changes, depicted at the bottom of Scheme 4, indicate that **TS3** can be viewed as the transition structure of an intramolecular hydrogen abstraction of the OH group by the radical center of the terminal oxygen, O1. As noted previously,[33] owing to the orthogonality between the singly occupied 2p-type orbital of oxygen O1 and the O–H bond in the reactant $^{\bullet}OOCH_2OH$, **TS4** adopts a puckered ring-like structure. This allows overlap between the 1s orbital of the hydrogen atom of the OH group and the singly occupied 2p-type orbital of oxygen O1.

Proton-coupled electron-transfer mechanism:

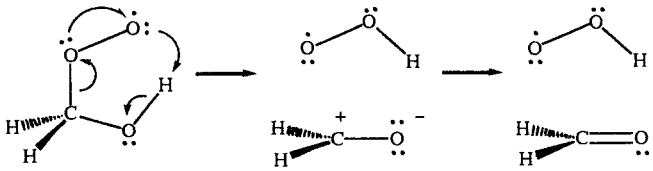

Hydrogen atom transfer mechanism:

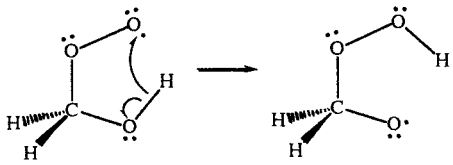

Scheme 4.

Conclusion

In this paper, we have investigated by means of quantum-mechanical electronic-structure calculations the intermolecular hydrogen atom transfer reaction $HCOOH + {}^{\bullet}OH \rightarrow HCOO^{\bullet} + H_2O$ and the intramolecular hydrogen-transfer reaction $^{\bullet}OOCH_2OH \rightarrow HOOCH_2O^{\bullet}$. Geometric structures for the reactants and transition states have been optimized at the UQCISD theory level with the 6-311+G(2df,2p) basis set. UCCSD(T) and RCCSD(T) energies were also calculated at the UQCISD-optimized geometries with the same basis set. In both reactions, we found that the hydrogen atom transfer can take place via two different transition structures that correspond to different reaction mechanisms. In each reaction, the lowest energy transition structure involves a proton transfer coupled to the transfer of an electron mechanism, whereas the higher energy transition structure corresponds to the conventional radical hydrogen abstraction mechanism. An analysis of the atomic spin populations, obtained within the framework of the topological theory of atoms in molecules, suggests that the triplet repulsion between the unpaired electrons located at the oxygen atoms undergoing the hydrogen exchange must be much higher in the transition structure for the radical hydrogen

atom abstraction than in the transition structure for the proton-coupled electron-transfer mechanism. It can be concluded that, in the gas phase, hydrogen atom transfer from hydroxylic oxygen to oxygen-centered radicals occurs preferentially by a proton-coupled electron-transfer mechanism rather than by radical hydrogen abstraction when both reaction mechanisms are possible.

Acknowledgments

This research was supported by the Spanish DGICYT (Grants BQU2002-04485-C02-01, BQU2002-04485-C02-02, and BQU2002-00293). Additional support came from Catalonian CIRIT (Grant 2001SGR00048). The larger calculations described in this work were performed on the CPQ AlphaServer HPC320 at the Centre de Supercomputació de Catalunya (CESCA). We are grateful to an anonymous referee for useful remarks, which served to clarify various points in the initial manuscript.

[1] For a review, see: R. Atkinson, *Atmos. Environ. Part A* **1990**, *24*, 1.
[2] J. Warnatz, In *Combustion Chemistry* (Ed.: W. C. Gardiner, Jr), Springer, New York, **1984**.
[3] a) A. A. A Zavitsas, *J. Am. Chem. Soc.* **1998**, *120*, 6578; b) A. A. Zavitsas, *J. Chem. Soc. Perkin trans. 2* **1996**, 391; c) A. A. Zavitsas, C. Chatgilialoglu, *J. Am. Chem. Soc.* **1995**, *117*, 10645; d) A. A. Zavitsas, A. A. Melikian, *J. Am. Chem. Soc.* **1975**, *97*, 2757; e) A. A. Zavitsas, *J. Am. Chem. Soc.* **1972**, *94*, 6578.
[4] a) L. Song, W. Wu, P. C. Hiberty, D. Danovich, S. Shaik, *Chem. Eur. J.* **2003**, *9*, 4540; b) L. Song, W. Wu, K. Dong, P. C. Hiberty, S. Shaik, *J. Phys. Chem. A* **2002**, *106*, 11361; c) S. Shaik, W. Wu, K. Dong, L. Song, P. C. Hiberty, *J. Phys. Chem. A* **2001**, *105*, 8226.
[5] a) M. Foti, K. U. Ingold, J. Lusztyk, *J. Am. Chem. Soc.* **1994**, *116*, 9440; b) L. R. Mahoney, M. A. DaRooge *J. Am. Chem. Soc.* **1975**, *97*, 4722.
[6] For recent reviews on proton-coupled electron-transfer reactions see: a) R. I. Cukier, D. G. Nocera, *Annu. Rev. Phys. Chem.* **1998**, *49*, 337–369; b) S. Hammes-Schiffer, *Acc. Chem. Res.* **2001**, *34*, 273–281; c) S. Hammes-Schiffer, *ChemPhysChem* **2002**, *3*, 22–42.
[7] The Cartesian coordinates of all structures reported in this paper are available in the Supporting Information.
[8] a) H. B. Schlegel, *J. Comput. Chem.* **1982**, *3*, 214; b) J. M. Bofill, *J. Comput. Chem.* **1994**, *15*, 1.
[9] J. A. Pople, M. Head-Gordon, K. Raghavachari, *J. Chem. Phys.* **1987**, *87*, 5968.
[10] M. J. Frisch, J. A. Pople, J. S. Binkley, *J. Chem. Phys.* **1984**, *80*, 3265.
[11] W. J. Hehre, L. Radom, P. von R. Schleyer, J. A. Pople, *Ab Initio Molecular Orbital Theory*, Wiley, New York, **1986**, pp. 86–87
[12] a) C. Moller, M. Plesset, *Phys. Rev.* **1934**, *46*, 618; b) J. A. Pople, J. S. Binkley, R. Seeger, *Int. J. Quantum Chem. Symp.* **1976**, *10*, 1.
[13] a) K. Ishida, K. Morokuma, A. Kormornicki, *J. Chem. Phys.* **1977**, *66*, 2153; b) C. Gonzalez, H. B. Schlegel, *J. Chem. Phys.* **1989**, *90*, 2154; c) C. Gonzalez, H. B. Schlegel, *J. Phys. Chem.* **1990**, *94*, 5523.
[14] Gaussian 98 (Revision A.7), M. J. Frisch, G. W. Trucks, H. B. Schlegel, G. E. Scuseria, M. A. Robb, J. R. Cheeseman, V. G. Zakrzewski, J. A. Montgomery, Jr., R. E. Stratmann, J. C. Burant, S. Dapprich, J. M. Millam, A. D. Daniels, K. N. Kudin, M. C. Strain, O. Farkas, J. Tomasi, V. Barone, M. Cossi, R. Cammi, B. Mennucci, C. Pomelli, C. Adamo, S. Clifford, J. Ochterski, G. A. Petersson, P. Y. Ayala, Q. Cui, K. Morokuma, D. K. Malick, A. D. Rabuck, K. Raghavachari, J. B. Foresman, J. Cioslowski, J. V. Ortiz, B. B. Stefanov, G. Liu, A. Liashenko, P. Piskorz, I. Komaromi, R. Gomperts, R. L. Martin, D. J. Fox, T. Keith, M. A. Al-Laham, C. Y. Peng, A. Nanayakkara, C. Gonzalez, M. Challacombe, P. M. W. Gill, B. G. Johnson, W. Chen, M. W. Wong, J. L. Andres, M. Head-Gordon, E. S. Replogle, J. A. Pople, Gaussian, Inc., Pittsburgh, PA, **1998**.
[15] For a review, see: R. J. Bartlett, *J. Phys. Chem.* **1989**, *93*, 1967.
[16] K. Raghavachari, G. W. Trucks, J. A. Pople, M. Head-Gordon, *Chem. Phys. Lett.* **1989**, *157*, 479.
[17] P. J. Knowles, C. Hampel, H.-J. Werner, *J. Chem. Phys.* **1993**, *99*, 5219.
[18] a) G. D. Purvis, R. J. Bartlett, *J. Chem. Phys.* **1982**, *76*, 1910; b) C. Hampel, K. A. Peterson, H.-J. Werner, *Chem. Phys. Lett.* **1992**, *190*, 1; c) M. J. O. Deegan, P. J. Knowles, *Chem. Phys. Lett.* **1994**, *227*, 321.
[19] H.-J. Werner, P. J. Knowles, J. Almlöf, R. D. Amos, A. Berning, D. L. Cooper, D. M. J. O. Deegan, A. J. Dobbyn. S. T. Eckert, C. Hampel, C. Leininger, R. Lindh, A. M. Lloyd, W. Meyer, M. E. Mura, A. Nicklass, P. Palmeiri, K. A. Peterson, R. Pitzer, P. Pulay, G. Rauhaut, M. Schütz, H. Stoll, A. J. Stone, T. Thorsteinsson, University of Stuttgart (Germany), **1998**.
[20] R. F. W. Bader, *Atoms in Molecules: A Quantum Theory*, Clarendon, Oxford, UK, **1990**.
[21] F. Mota, Universitat de Barcelona, unpublished work.
[22] a) F. W. Biegler-König, R. F. W. Bader, T.-H. Tang, *J. Comput. Chem.* **1982**, *3*, 317; b) R. F. W. Bader, T.-H. Tang, Y. Tal, F. W. Biegler-König, *J. Am. Chem. Soc.* **1982**, *104*, 946.
[23] See, for example: K. B. Wiberg, C. M. Hadad, T. LePage, C. M. Breneman, M. J. Frisch, *J. Phys. Chem.* **1992**, *96*, 671.
[24] A. A. Nanayakkara, G. G. Balint-Kurti, I. H. Williams, *J. Phys. Chem.* **1992**, *96*, 3662.
[25] H. Basch, S. Hoz, *J. Phys. Chem. A* **1997**, *101*, 4416.
[26] M. R. Hand, C. F. Rodriguez, I. H. Williams, G. G. Balint-Kurti, *J. Phys. Chem. A* **1998**, *102*, 5958.
[27] L. Masgrau, A. Gonzalez-Lafont, J. M. Lluch, *J. Phys. Chem. A* **1999**, *103*, 1044.
[28] H-J. Deyerl, A. K. Luong, T. G. Clements, R. E. Continentti, *Faraday Discuss.* **2000**, *115*, 147.
[29] T. Uchimaru, A. K. Chandra, S. Tsuzuki, M. Sugie, A. Sekiya, . *J. Comput. Chem.* **2003**, 1538–1548.
[30] The total energies and ZPVEs are collected in Table S1 (Supporting Information). Calculated topological properties of the bond critical points for the transition structure are given in Table S2 (Supporting Information). As expected, the geometrical parameters calculated for the transition structure of Equation (5) (Figure 1) are comparable to the values reported in the previous theoretical investigations. In particular, bond lengths, bond angles, and dihedral angles differ by less than 0.002 Å, 1.4°, and 0.7°, respectively, from the values reported by Uchimaru et al.,[29] calculated at the UQCISD theory level with the 6-3111++G(3d,2p) basis set.
[31] M. K. Dubey, R. Mohrschladt, N. M. Donahue, J. G. Anderson, *J. Phys. Chem. A* **1997**, *101*, 1494.
[32] A. Galano, J. R. Alvarez-Idaboy, M. E. Ruiz-Santoyo, A. Vivier-Bunge, *J. Phys. Chem. A* **2002**, *106*, 9520–9528.
[33] S. Olivella, J. M. Bofill, A. Sole, *Chem. Eur. J.* **2001**, *7*, 3377–3386.

Received: November 13, 2003
Revised: February 25, 2004
Published online: May 24, 2004

